Improving High Efficiency and Device Lifetime of Blue Emitters with 3H-Benzo[cd]Pyrene Core and Optimized Bulky Side Groups

Hyukmin Kwon[a,1], Sunwoo Park[a], Seokwoo Kang[a], Sangwook Park[a], Kiho Lee[a], Hayoon Lee[a], and Jongwook Park[a]*

[a]Intergrated Engineering, Department of Chemical Engineering, Kyung Hee University, Gyeonggi, 17104, Korea

General information

Reagents and solvents were purchased as reagent grade and were used without further purification. Analytical TLC was carried out on a Merck 60 F254 silica gel plate, and column chromatography was performed on Merck 60 silica gel (230-400 mesh). The 1H-NMR spectra were recorded on Bruker Advance 300 spectrometers. The FAB+-mass and EI+-spectra were recorded on a JMS-600W, JMS-700, 6890 Series, and Flash1112 or Flash2000. The optical UV-Vis absorption spectra were obtained using a Lambda 1050 UV/Vis/NIR spectrometer (Perkin Elmer). A Perkin-Elmer luminescence spectrometer LS55 (Xenon flash tube) was used to perform PL spectroscopy. The glass transition temperatures (T_g) and melting temperatures (T_m) of the compounds were obtained on a Differential Scanning Calorimetry (DSC) Discovery DSC25 (TA instruments) under a nitrogen atmosphere. Compounds were heated to 300 ℃ at rate of 5 ℃/min and cooled at 5 ℃/min. Degradation temperatures (T_d) values of the compounds were measured with Thermal Gravimetric Analysis (TGA) using a TGA4000 (Perkin Elmer). Samples were heated to 700 ℃ at a rate of 10 ℃/min. The HOMO energy levels were determined with ultraviolet photoelectron spectroscopy (Riken Keiki AC-2). The LUMO energy levels were derived from the HOMO energy levels and the band gaps. Cyclic voltammograms were recorded with a Potentionstat/Galvanostat Model 273A(Princeton Applied Research). For the EL devices, all organic layers were deposited under 10^{-6} torr, with a rate of deposition of 1 Å/s to give a deposition area of 4 mm^2. The LiF and aluminum layers were continuously deposited under the same vacuum condition. The current-voltage-luminance (J-V-L) characteristics of the fabricated EL devices were obtained with a Keithley 2400 electrometer. Light intensities were obtained with a Minolta CS-1000A. The transient electroluminescence (TrEL) was carried out at 10 mA/cm^2. The aspect ratio of pulse applied from the 33600A function generator (KEYSIGHT) is 1:1, and the pulse width is 500 us.

Device fabrication

In each of the OLED devices, dipyrazino[2,3-f:2',3'-h]quinoxaline-2,3,6,7,10,11-hexacarbonitrile (HAT-CN) were used for the hole injection layer (HIL), N4,N4,N4',N4'-Tetra[(1,1'-biphenyl)-4-yl]-(1,1'-biphenyl)-4,4'-diamine (BPBPA) were used for the hole transporting layer (HTL), N-([1,1'-biphenyl]-4-yl)-N-(9,9-dimethyl-9H-fluoren-2-yl)spiro[benzo[de]anthracene-7,9'-fluoren]-4'-amine (BPACz) was used for the electron blocking and hole transporting layer (EBL-HTL), 9-(naphthalen-1-yl)-10-(naphthalen-2- S-4yl)anthracene (α,β-ADN) was used for the host material in emitting layer (EML), DMP-BP and DBF-BP were used as the dopant material in EML, DNAPBi, and 8-quinolinolato lithium (Liq) were used for the electron transporting layer (ETL), lithium fluoride (LiF) was used for the electron injection layer (EIL), ITO was used as the anode, and Al was used as the cathode. All organic layers were deposited under 10^{-6} Torr, with a rate of deposition of 1 Å s^{-1} to create an emitting area of 4 mm^2. The LiF and Al layers were continuously deposited under the same vacuum conditions. The EL performances of fabricated OLED devices were obtained by using a Keithley 2400 electrometer. Light intensities were obtained using a Minolta CS-1000A spectroradiometer. The operational stabilities of the devices were measured after encapsulation in a glove box.

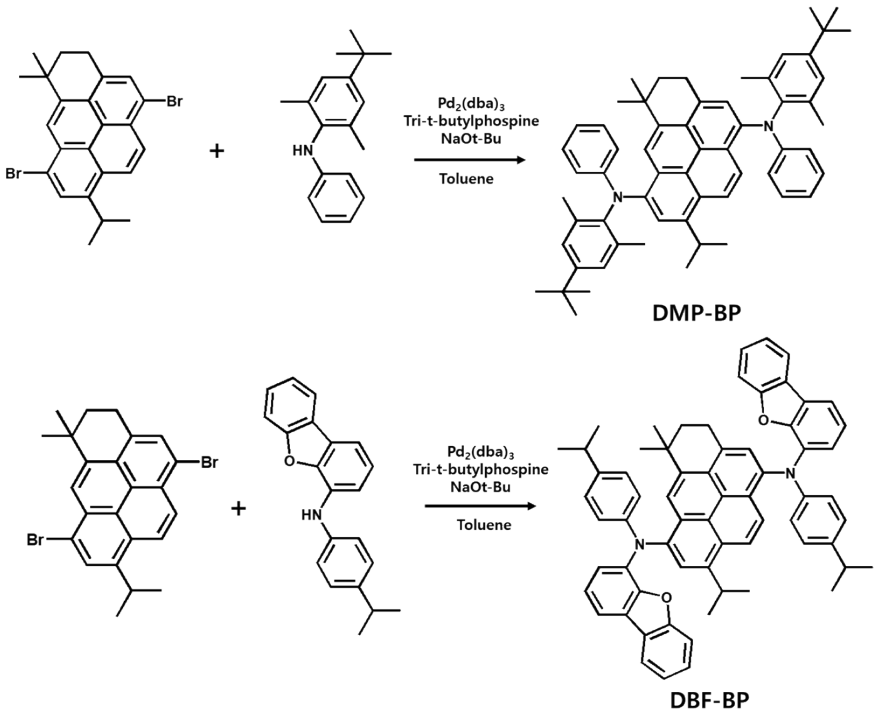

Scheme S1. Synthetic routes of newly synthesized materials.

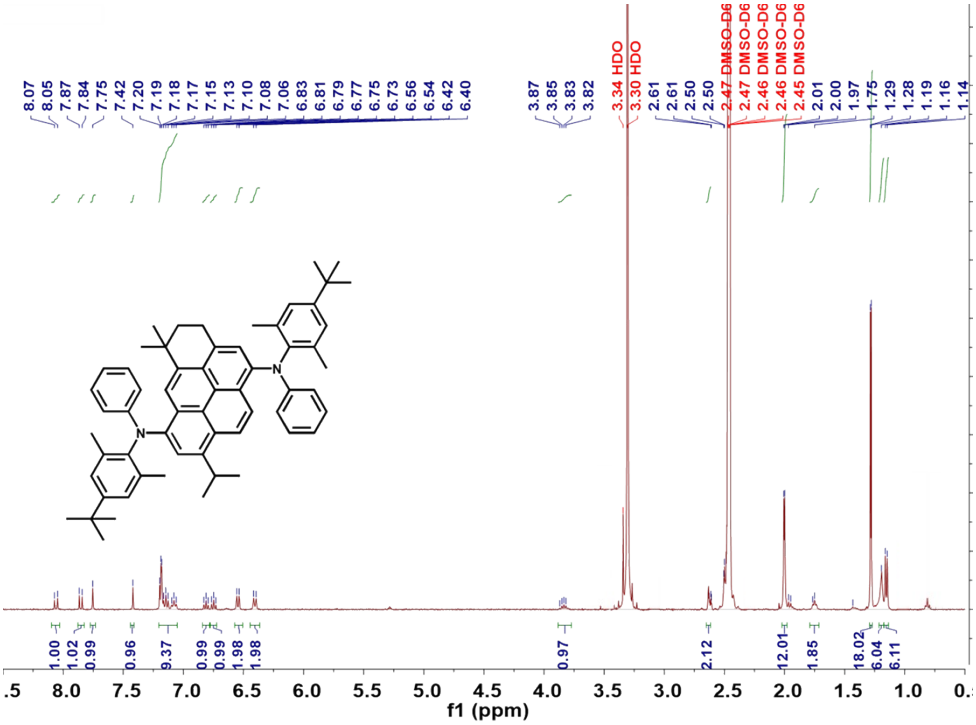

Fig. S1. [1]H-NMR spectrum of DMP-BP.

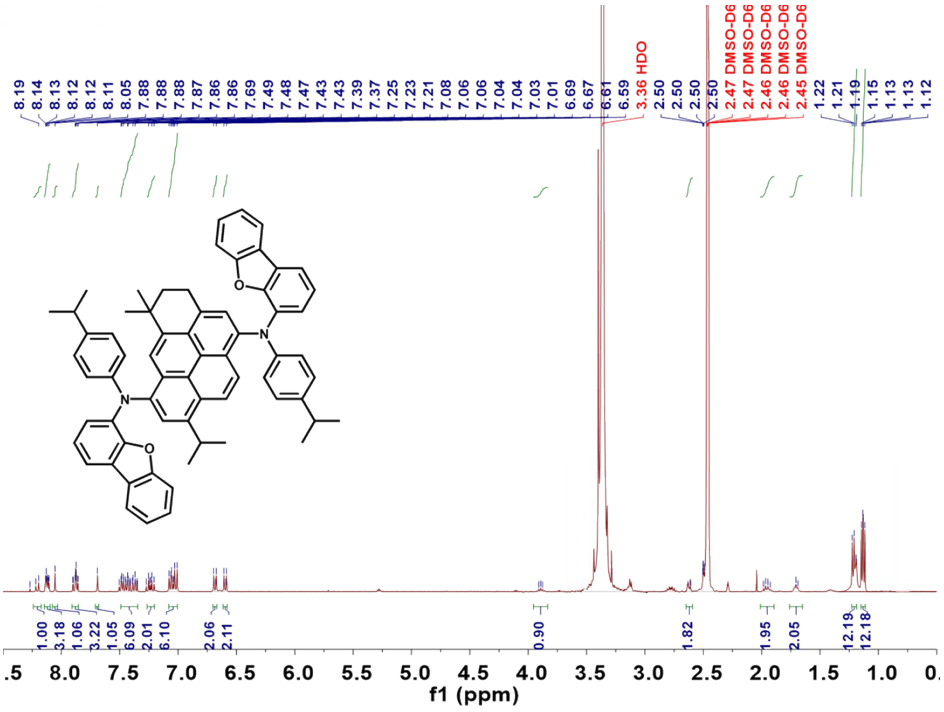

Fig. S2. [1]H-NMR spectrum of DBF-BP.

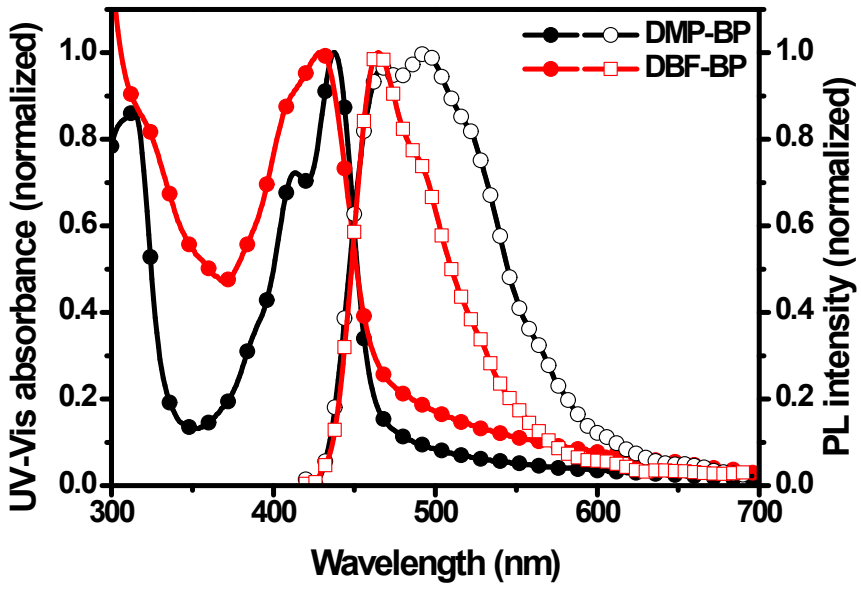

Fig. S3. UV–vis absorption and PL spectra of benzo[cd]pyrene derivatives in film state (thickness: 50nm).

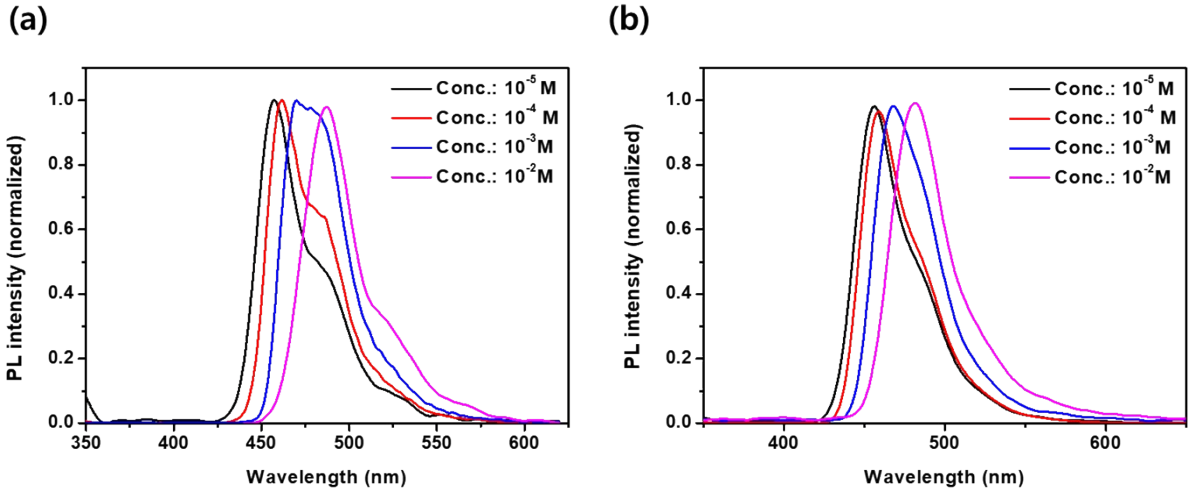

Fig. S4. PL spectra according to concentration in solution states (a) DMP-BP and (b) DBF-BP.

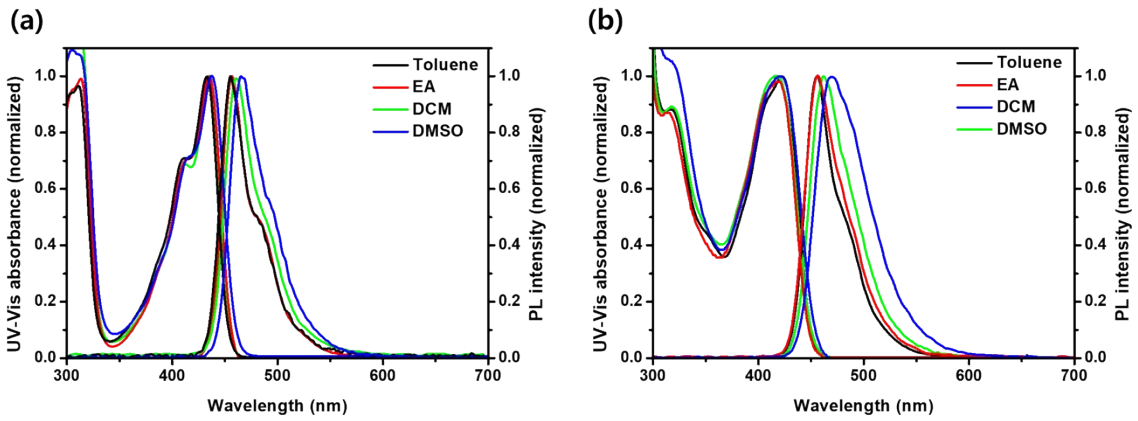

Fig. S5. UV absorbance and PL spectra of (a) DMP-BPP and (b) DBF-BP in various solvents.

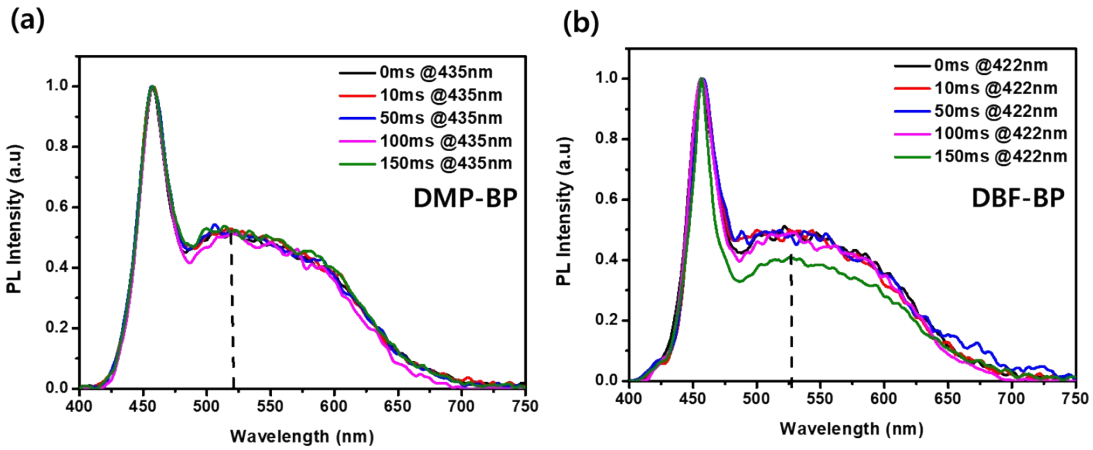

Fig. S6. PL spectra of the synthesized compounds in toluene solution (10^{-5}M) at 77 K. (a) DMP-BP and (b) DBF-BP.

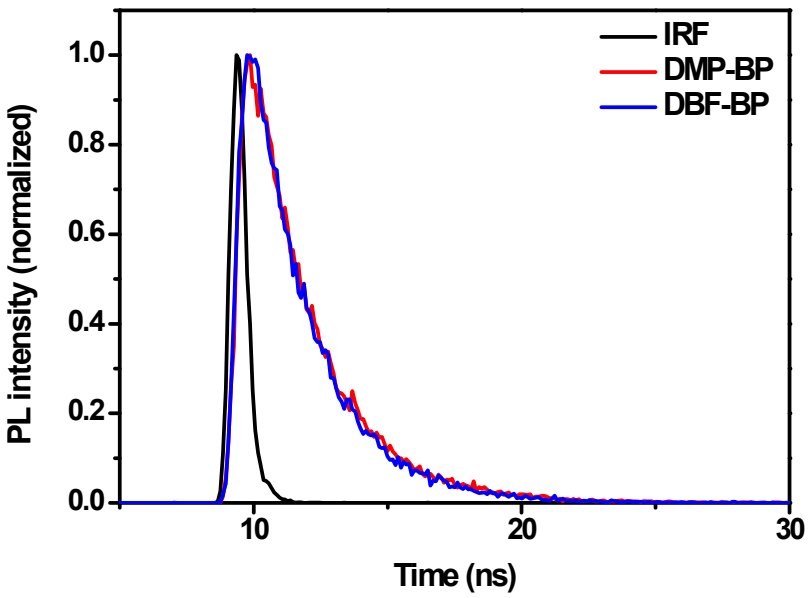

Fig. S7. Transient PL decay profiles of DMP-BP and DBP-BP in solution state.

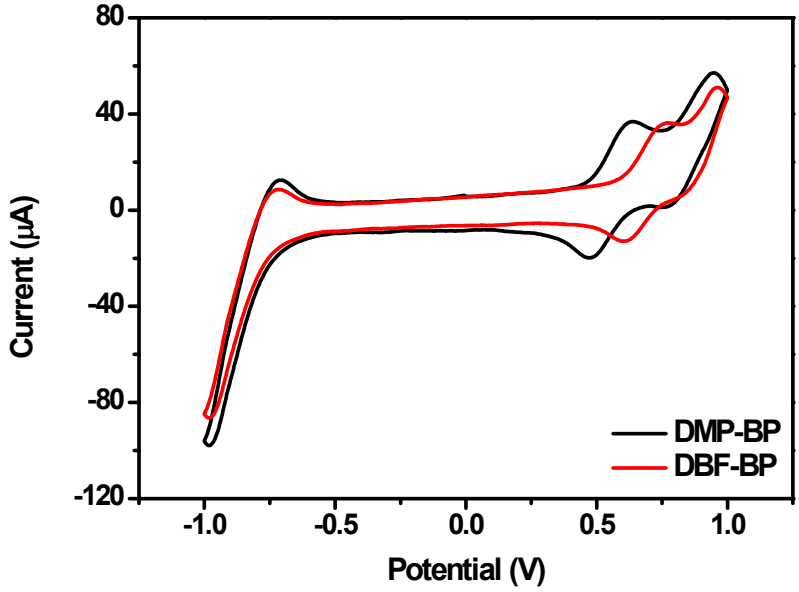

Fig S8. Cyclic voltammograms under 100 mV/s of DMP-BP and DBF-BP [0.1 M TBAP-F6 in dichloromethane].

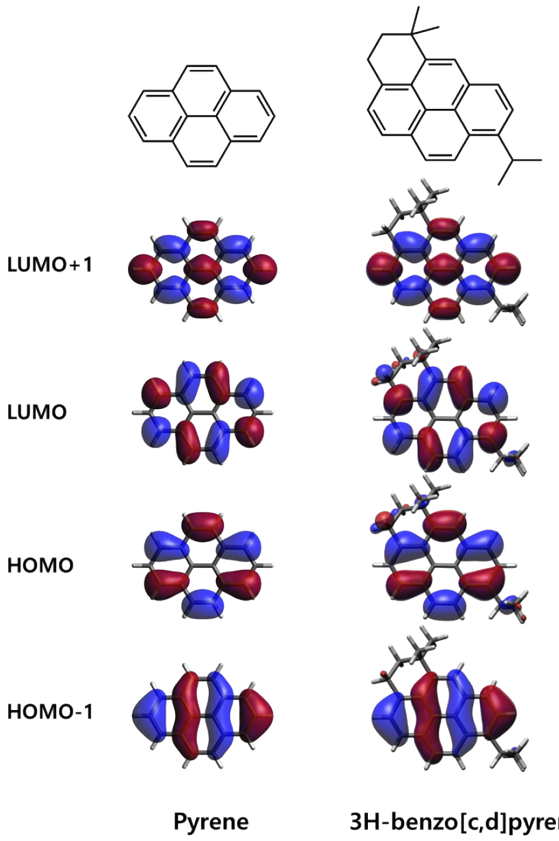

Fig. S9. HOMO−1, HOMO, LUMO and LUMO+1 electronic density distributions of the S_0 states of the pyrene and 3H-benzo[c,d]pyrene calculated at the B3LYP/6-31G(d).

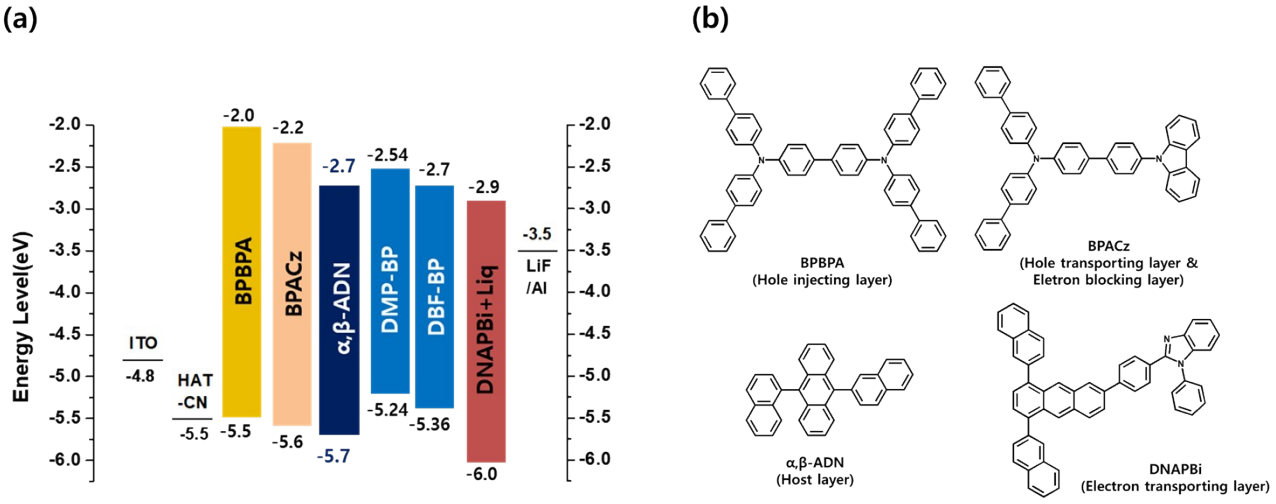

Fig. S10. (a) Band diagrams of the fabricated OLED devices, (b) chemical structures of materials used for OLED devices fabrication.

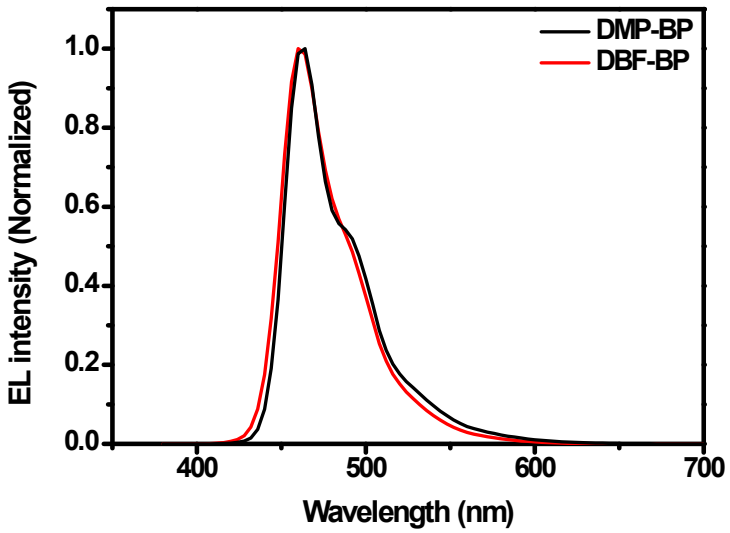

Fig. S11. EL spectra of fabricated OLED devices.

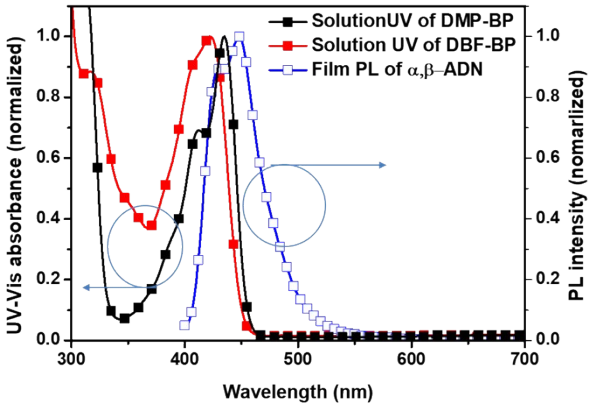

Fig. S12. Spectral overlap between the absorption of DMP-BP and DBF-BP and the photoluminescence of α,β-ADN host material.

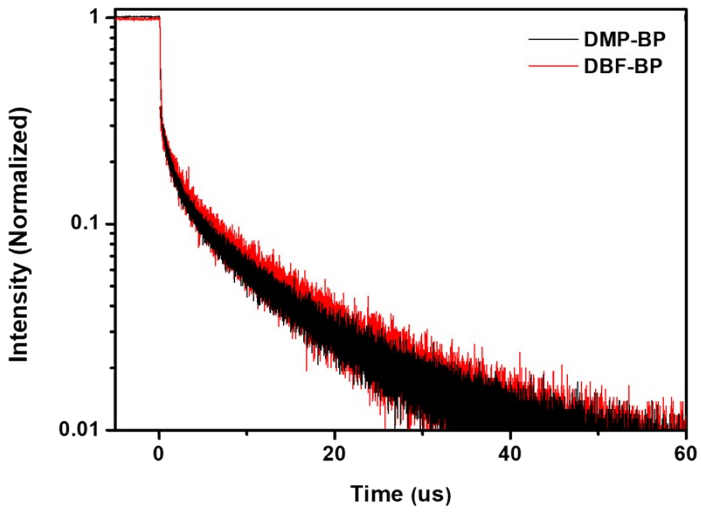

Fig. S13. Transient EL decay of non-doped devices of DMP-BP and DBF-BP.

Table S1. Summary of TD-DFT calculation results of pyrene and BP core materials calculated at the B3LYP/6-31G(d,p).

Materials	HOMO (eV)	LUMO (eV)	S_1	T_1	ΔE_{ST} [a]	λ_{abs} (nm) (oscillator strength (f))	Characteristic transition	Contribution (%)
Pyrene	-5.66	-1.83	3.76	2.43	1.89	321 (0.2994)	H-1 → L+1/ H → L	15.6/80.4
BP core	-5.32	-1.59	3.67	2.38	1.90	331 (0.3615)	H-1 → L+1/ H → L	11.5/72.7

[a] $\Delta E_{ST} = S_1 - T_1$. [b] Oscillator strength

Table S2. Thermal properties of the synthesized materials.

Materials	T_g[a] (℃)	T_d[c] (℃)
DMP-BP	154	432
DBF-BP	184	441

[a] Glass transition temperature. [b] Decomposition temperature at 5% weight loss.